Available online at www.sciencedirect.com
SCIENCE DIRECT®
ELSEVIER
International Journal of Solids and Structures 42 (2005) 2741–2754
INTERNATIONAL JOURNAL OF SOLIDS and STRUCTURES
www.elsevier.com/locate/ijsolstr

Deformation and stress analysis of circumferentially fiber-reinforced composite disks

M. Tahani [a,*], A. Nosier [b], S.M. Zebarjad [c]

[a] Department of Mechanical Engineering, Faculty of Engineering, Ferdowsi University of Mashhad, Mashhad, Iran
[b] Department of Mechanical Engineering, Sharif University of Technology, Azadi Ave., Tehran, Iran
[c] Department of Materials Science and Metallurgy, Faculty of Engineering, Ferdowsi University of Mashhad, Mashhad, Iran

Received 1 May 2004; received in revised form 26 September 2004

Abstract

A semi-analytical method is developed for the analysis of deformation and three-dimensional stress field in rotating annular disks made of cylindrically orthotropic nested rings. The method is based on a layerwise theory and the Hamilton principle. The proposed method is applied to calculate in-plane and out-of-plane stresses in a rotating disk made up of two nested rings that is rigidly fixed (or free) at the inner boundary and is free at the outer boundary. The computed results are compared with those obtained from the finite element method. It is found that because of discontinuity of material properties, the stress field is three-dimensional at the interface of two rings.

Keywords: Composite materials; Rotating disk; Cylindrical orthotropic; Stress field

1. Introduction

Rotating disks have a wide range of applications as energy storage devices and for gyroscopic control of ships, submarines, aircrafts, rockets, and missiles. Also rotating disks have engineering applications such as high-speed gears and turbine rotors.

Contrary to the aforementioned numerous applications, little research effort has been devoted so far for development of the theoretical or numerical models for predicting accurate stress analysis in rotating disks.

* Corresponding author. Tel.: +98 511 882 9538; fax: +98 511 882 9541.
E-mail address: mtahani@ferdowsi.um.ac.ir (M. Tahani).

0020-7683/$ - see front matter
doi:10.1016/j.ijsolstr.2004.09.041

Timoshenko and Goodier (1970) analyzed a constant-thickness rotating isotropic disk as a three-dimensional problem. Lekhnitskii (1981), Reddy and Srinath (1974), Gurushankar (1975), Christensen and Wu (1977), and Genta and Gola (1981) determined stresses by using elasticity approaches in orthotropic single-ply circular plates with stress-free outer boundary. Bert (1975) used a classical lamination theory on layered plates with extension-bending coupling and with stress-free boundaries. Tutuncu (1995) obtained stresses and deformations resulting from centrifugal forces in rotating especially orthotropic circular plates using the classical lamination theory to illustrate the effect of anisotropy on stresses. Although the symmetric cross-ply and balanced laminates were considered, the displacement field was only function of the radial coordinate. Furthermore, Tutuncu (1998) analyzed interlaminar stresses in generally polar-anisotropic circular plates due to the uniform change in temperature. It is to be noted that the analysis was based on the plane stress state assumptions with rotational symmetry. Tutuncu (1998) showed that increasing in the number of circumferentially wound laminae increased the strength of the laminate against thermal loads. Durodola and Attia (2000) studied the potential benefits of using fiber-reinforced functionally graded materials for rotating hollow and solid disks. Jain et al. (2000) studied singularity in rotating polarly orthotropic disks, shallow shells, and conical shells. They (Jain et al., 2000) observed that there is no singularity when the ratio of tangential to radial modulus of elasticity is equal or greater than one.

Recently Arnold et al. (2002) analyzed the problem of a rotating disk in the form of a single disk or a number of concentric disks forming a unit. Their analytical model is capable of performing an elastic stress analysis for various disk systems subjected to pressure surface tractions, body forces, and interfacial misfits. They (Arnold et al., 2002) presented key design variables of disk systems and their associated influence. It should be mentioned here that the analysis was performed based on the plane stress assumption.

Foral and Newhouse (1980) investigated the performance of hoop wound composite flywheel rotors. Performance measurements used in this study were energy stored per unit swept volume, per unit rotor weight, and per unit material cost. They explained that of the many configurations available in composite rotor design, a very attractive, easily fabricated one is the simple hoop wound rotor, with continuous filaments circumferentially wound in an epoxy matrix. Moreover, they mentioned that an additional approach uses a multiple material design where the rotor is constructed with nested circumferential rings, each with a different structural material. Properly selected material combinations can produce significantly increase in energy storage capacity.

It is well known that the stress field is three-dimensional (3-D) in regions of geometrical or material discontinuities. Based on the results obtained by Tutuncu (1998) and Foral and Newhouse (1980), the present study deals with a semi-analytical solution of 3-D stress field in disks constructed with nested circumferentially fiber-reinforced composite rings. It is assumed that at the inner boundary the plate is fixed (or free) and at the outer boundary is free of stress. To obtain accurate results, a layerwise theory (LWT) is used to model the problem. The results obtained from this theory will be compared with those obtained by using the finite element method.

2. Theoretical formulation

As it is pointed out, based on the work done by Tutuncu (1998) and Foral and Newhouse (1980), of the many configurations available in composite rotor design, a very attractive, easily fabricated one is the simple hoop wound rotor, with continuous filaments circumferentially wound in an epoxy matrix. Therefore, it is intended here to accurately determine the full 3-D stress distribution in circumferentially wound disks with inner and outer radii $R_I(\equiv R_1)$ and $R_0(\equiv R_{M+1})$, respectively, rotating with a constant angular velocity ω. The disk is made up of M discrete, nested rings, each with inner and outer radii R_i and R_{i+1}, respectively, and of a single specified material of mass density ρ_i (see Fig. 1).

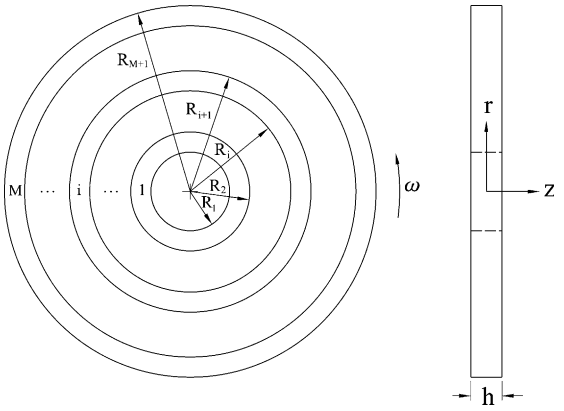

Fig. 1. Schematic of M concentric annular disks.

2.1. Displacement field and strains

As mentioned previously, the full layerwise laminate theory of Reddy (see, e.g., Nosier et al., 1993; Tahani and Nosier, 2004) is used to obtain accurate 3-D stress field in the disk. The displacement field in this theory may be written as

$$\begin{aligned} u_r(r,\theta,z,t) &= U_k(r,t)\Phi_k(z) \\ u_\theta(r,\theta,z,t) &= 0 \qquad\qquad k=1,2,\ldots,N+1 \\ u_z(r,\theta,z,t) &= W_k(r,t)\Phi_k(z) \end{aligned} \tag{1}$$

where, for the sake of brevity, the Einstein summation convention has been introduced-a repeated index indicates summation over all values of that index. In Eqs. (1) u_r, u_θ, and u_z represent the displacement components in the r, θ, and z directions, respectively, of a material point located at (r, θ, z) in the undeformed disk (see Fig. 1). Also $U_k(r, t)$ and $W_k(r, t)$ $(k = 1, 2, \ldots, N + 1)$ represent the displacement components of all points located on the kth numerical plane in the r and z directions, respectively, in the undeformed disk and $\Phi_k(z)$ are continuous functions of the thickness coordinate z (global interpolation functions). For linear variation through each numerical layer these functions are defined as

$$\Phi_k(z) = \begin{cases} 0 & z \leqslant z_{k-1} \\ \phi^2_{k-1}(z) & z_{k-1} \leqslant z \leqslant z_k \\ \phi^1_k(z) & z_k \leqslant z \leqslant z_{k+1} \\ 0 & z \geqslant z_{k+1} \end{cases} \qquad k=1,2,\ldots,N+1 \tag{2}$$

In Eq. (2) ϕ^j_k $(j = 1, 2)$ is the local (i.e. layer) linear Lagrangian interpolation function associated with the jth node of the kth layer that defined as

$$\phi^1_k = \frac{z_{k+1}-z}{h_k}, \quad \phi^2_k = \frac{z-z_k}{h_k} \tag{3}$$

where h_k is the thickness of the kth numerical layer and z_k denotes the z-coordinate of the bottom of the kth numerical layer. In this model, it is assumed that a ring is constructed of N numerical (or mathematical) layers with the same material properties. Clearly, as the number of numerical layers is increased, the accuracy of the results in the z direction is also increased. It is worth noting that, since the rings are

circumferentially wound the problem is an axisymmetric one and, therefore, there is no displacement in the θ direction. Hence, all the functions appear in Eqs. (1) are independent of variable θ.

Upon substitution of Eqs. (1) into the linear strain–displacement relations (Fung, 1965) of elasticity, the following results will be obtained:

$$\begin{aligned} &\varepsilon_r = \frac{\partial U_k}{\partial r}\Phi_k, \quad \varepsilon_\theta = \frac{1}{r}U_k\Phi_k, \quad \varepsilon_z = W_k\frac{\mathrm{d}\Phi_k}{\mathrm{d}z} \\ &\varepsilon_{r\theta} = \varepsilon_{\theta z} = 0, \quad \varepsilon_{rz} = \frac{1}{2}\left(U_k\frac{\mathrm{d}\Phi_k}{\mathrm{d}z} + \frac{\partial W_k}{\partial r}\Phi_k\right) \end{aligned} \tag{4}$$

It is to be noted that the strains in Eq. (2) are discontinuous at the layer interfaces because of the layerwise definition of the functions $\Phi_k(z)$. Hence, the theory assumes separate displacement field expansions within each material layer that exhibits only C^0-continuity through the thickness of the circular plate. Therefore, the resulting strain field is kinematically correct specially when the number of numerical layers is increased. Thus the in-plane strains are continuous through the laminate thickness and at the same time the transverse strains are piecewise continuous at the ply interfaces. That is, it is possible in this theory to analyze hoop wound composite disks constructed with nested circumferential rings and at the same time each ring could be laminated by different materials.

2.2. Equations of motion

The Hamilton principle for an elastic body is (Fung, 1965):

$$\int_{t_1}^{t_2}(\delta U + \delta V - \delta T)\,\mathrm{d}t = 0 \tag{5}$$

where δU is the variation of the total strain energy, δV is the variation of the potential energy of the applied forces on the external surfaces of the disk, and δT is the variation of the total kinetic energy. That is

$$\begin{aligned} \delta U &= 2\pi\int_{R_i}^{R_{i+1}}\int_{-h/2}^{h/2}(\sigma_r\delta\varepsilon_r + \sigma_\theta\delta\varepsilon_\theta + \sigma_z\delta\varepsilon_z + 2\sigma_{rz}\delta\varepsilon_{rz})r\,\mathrm{d}z\,\mathrm{d}r \\ &= -2\pi\int_{R_i}^{R_{i+1}}\left\{[(rM_r^k)_{,r} - M_\theta^k - rQ_r^k]\delta U_k + [(rR_r^k)_{,r} - rN_z^k]\delta W_k\right\}\mathrm{d}r + 2\pi\left[rM_r^k\delta U_k\right]_{r=R_i}^{r=R_{i+1}} \\ &\quad + 2\pi\left[rR_r^k\delta W_k\right]_{r=R_i}^{r=R_{i+1}} \end{aligned} \tag{6}$$

where the generalized stress resultants are defined as

$$\begin{aligned} &(M_r^k, M_\theta^k, R_r^k) = \int_{-h/2}^{h/2}(\sigma_r, \sigma_\theta, \sigma_{rz})\Phi_k\,\mathrm{d}z \\ &(N_z^k, Q_r^k) = \int_{-h/2}^{h/2}(\sigma_z, \sigma_{rz})\frac{\mathrm{d}\Phi_k}{\mathrm{d}z}\,\mathrm{d}z \end{aligned} \tag{7}$$

It is to be noted that in the layerwise theory each physical layer can be divided into a number of numerical layers and within each numerical layer, on the other hand, the quantities M_r^k and M_θ^k do, in fact, represent moments. For this reason, in this study, the symbol M is used for the generalized stress resultants M_r^k and M_θ^k. Also δV is given by

$$\delta V = -\int_\Gamma\int_{-h/2}^{h/2}(\bar{\sigma}_r\delta u_r + \bar{\sigma}_{rz}\delta u_z)\,\mathrm{d}z\,\mathrm{d}s \tag{8}$$

where $\bar{\sigma}_r$ and $\bar{\sigma}_{rz}$ are the specified stress components on the inner and outer boundaries of the disk. Substituting for δu_r and δu_z from Eqs. (1) into Eq. (8) results in

$$\delta V = -2\pi \int_{-h/2}^{h/2} r(\bar{\sigma}_r \Phi_k \delta U_k + \bar{\sigma}_{rz} \Phi_k \delta W_k)|_{r=R_i}^{r=R_{i+1}} \,\mathrm{d}z = -2\pi \left[r\overline{M}_r^k \delta U_k \right]_{r=R_i}^{r=R_{i+1}} - 2\pi \left[r\overline{R}_r^k \delta W_k \right]_{r=R_i}^{r=R_{i+1}} \tag{9}$$

It is to be noted that here $\overline{M}_r^k$ and $\overline{R}_r^k$ are obtained by substituting $\sigma_r (\equiv \bar{\sigma}_r)$ and $\sigma_{rz} (\equiv \bar{\sigma}_{rz})$, respectively, into the definitions of stress resultants M_r^k and R_r^k as given in Eqs. (7).

Next, in order to obtain δT, the position vector of a material point in cylindrical coordinate and its time derivative (i.e., velocity) are noted to be

$$\vec{r} = (r + u_r)\vec{e}_r + (z + u_z)\vec{e}_z, \quad \vec{v} = \dot{u}_r \vec{e}_r + (r + u_r)\omega \vec{e}_\theta + \dot{u}_z \vec{e}_z \tag{10}$$

Since it is assumed that the disk rotates with a constant angular velocity (or the angular velocity is increased slowly), the problem is not time dependent and the variation of the total kinetic energy can be written as

$$\begin{aligned} \int_{t_1}^{t_2} \delta T \,\mathrm{d}t &= 2\pi \int_{t_1}^{t_2} \int_{R_i}^{R_{i+1}} \int_{-h/2}^{h/2} \rho_i (v_r \delta v_r + v_\theta \delta v_\theta + v_z \delta v_z) r \,\mathrm{d}r \,\mathrm{d}z \,\mathrm{d}t \\ &= 2\pi \int_{t_1}^{t_2} \int_{R_i}^{R_{i+1}} (\overline{I}^k r\omega^2 \delta U_k + \overline{I}^{kj} \omega^2 U_j \delta U_k) r \,\mathrm{d}r \,\mathrm{d}t \end{aligned} \tag{11}$$

where

$$(\overline{I}^k, \overline{I}^{kj}) = \int_{-h/2}^{h/2} \rho_i (\Phi_k, \Phi_k \Phi_j) \,\mathrm{d}z \tag{12}$$

Lastly, substituting Eqs. (6), (9), and (11) into Hamilton's principle in Eq. (5) yields the equations of motion for the ith ring:

$$\begin{aligned} &\delta U_k : \frac{\mathrm{d}M_r^k}{\mathrm{d}r} + \frac{M_r^k - M_\theta^k}{r} - Q_r^k = -\overline{I}^k r\omega^2 - \overline{I}^{kj} U_j \omega^2 \\ &\delta W^k : \frac{\mathrm{d}R_r^k}{\mathrm{d}r} + \frac{1}{r} R_r^k - N_z^k = 0 \end{aligned} \tag{13}$$

The primary variables (i.e., generalized displacements) and secondary variables (i.e., generalized forces) of the present LWT are:

$$\begin{aligned} &\text{Primary variables :} \quad U_k, W_k \\ &\text{Secondary variables :} \quad rM_r^k, rR_r^k \end{aligned} \tag{14}$$

It is noted that, when the disk becomes extremely thin, the radial displacement becomes constant through the thickness of the disk. In such a case it suffices to model the physical layer by one numerical layer. In other words, is such a case Eqs. (13) will represent two equations which when added to each other will give us the classical equilibrium equation (which is based on the assumption of radial displacement being constant through the thickness).

In order to find the displacement equations of motion, it is assumed that the disk is constructed with cylindrical orthotropic rings. The linear constitutive relations for the kth orthotropic lamina with respect to the disk coordinate axes (see Fig. 1) are given by (Herakovich, 1998):

$$\begin{Bmatrix} \sigma_\theta \\ \sigma_r \\ \sigma_z \\ \sigma_{rz} \\ \sigma_{\theta z} \\ \sigma_{r\theta} \end{Bmatrix}^{(k)} = \begin{bmatrix} C_{11} & C_{12} & C_{13} & 0 & 0 & 0 \\ C_{12} & C_{22} & C_{23} & 0 & 0 & 0 \\ C_{13} & C_{23} & C_{33} & 0 & 0 & 0 \\ 0 & 0 & 0 & C_{44} & 0 & 0 \\ 0 & 0 & 0 & 0 & C_{55} & 0 \\ 0 & 0 & 0 & 0 & 0 & C_{66} \end{bmatrix}^{(k)} \begin{Bmatrix} \varepsilon_\theta \\ \varepsilon_r \\ \varepsilon_z \\ 2\varepsilon_{rz} \\ 2\varepsilon_{\theta z} \\ 2\varepsilon_{r\theta} \end{Bmatrix}^{(k)} \tag{15}$$

where $C_{ij}^{(k)}$ are the material stiffnesses of the kth layer. It is noted that if each ring is constructed of a single material, we have N numerical layers through the thickness with the same material properties. Upon substitution of Eqs. (4) into (15) and the subsequent results into Eqs. (7), the stress resultants are obtained which can be presented as follows:

$$\begin{aligned} (N_z^k, M_r^k, M_\theta^k) &= (B_{13}^{jk}, D_{11}^{kj}, D_{12}^{kj})U_{j,r} + \frac{1}{r}(B_{23}^{jk}, D_{12}^{kj}, D_{22}^{kj})U_j + (A_{33}^{jk}, B_{13}^{kj}, B_{23}^{kj})W_j \\ (Q_r^k, R_r^k) &= (A_{55}^{kj}, B_{55}^{kj})U_j + (B_{55}^{jk}, D_{55}^{kj})W_{j,r} \end{aligned} \tag{16}$$

where the rigidity terms are given by

$$(A_{pq}^{kj}, B_{pq}^{kj}, D_{pq}^{kj}) = \sum_{i=1}^{N} \int_{z_i}^{z_{i+1}} C_{pq}^{(i)} \left(\frac{\mathrm{d}\Phi_k}{\mathrm{d}z}\frac{\mathrm{d}\Phi_j}{\mathrm{d}z}, \Phi_k \frac{\mathrm{d}\Phi_j}{\mathrm{d}z}, \Phi_k \Phi_j \right) \mathrm{d}z \tag{17}$$

Finally, substituting Eqs. (16) into Eqs. (13) yields $2(N+1)$ equations of motion corresponding to $2(N+1)$ unknowns U_j and W_j:

$$\begin{aligned} &D_{11}^{kj}\frac{\mathrm{d}^2U_j}{\mathrm{d}r^2} + \frac{1}{r}D_{11}^{kj}\frac{\mathrm{d}U_j}{\mathrm{d}r} - \left(\frac{1}{r^2}D_{22}^{kj} + A_{55}^{kj}\right)U_j + (B_{13}^{kj} - B_{55}^{jk})\frac{\mathrm{d}W_j}{\mathrm{d}r} + \frac{1}{r}(B_{13}^{kj} - B_{23}^{kj})W_j = -(\bar{I}^k r + \bar{I}^{kj}U_j)\omega^2 \\ &(B_{55}^{kj} - B_{13}^{jk})\frac{\mathrm{d}U_j}{\mathrm{d}r} + \frac{1}{r}(B_{55}^{kj} - B_{23}^{jk})U_j + D_{55}^{kj}\frac{\mathrm{d}^2W_j}{\mathrm{d}r^2} + \frac{1}{r}D_{55}^{kj}\frac{\mathrm{d}W_j}{\mathrm{d}r} - A_{33}^{kj}W_j = 0 \end{aligned} \tag{18}$$

3. Semi-analytical solutions

Here, in this section, a semi-analytical method will be used for solving Eqs. (18). In this method, each physical ring is divided into a large number of numerical (or mathematical) rings and it is assumed that the variable coefficients in Eqs. (18) are constant in each numerical ring (see Fig. 2). This way, Eqs. (18) for the m th numerical ring may be written as follows:

$$\begin{aligned} &D_{11}^{kj}\frac{\mathrm{d}^2U_j}{\mathrm{d}r^2} + \frac{1}{r_m}D_{11}^{kj}\frac{\mathrm{d}U_j}{\mathrm{d}r} - \left(\frac{1}{r_m^2}D_{22}^{kj} + A_{55}^{kj}\right)U_j + (B_{13}^{kj} - B_{55}^{jk})\frac{\mathrm{d}W_j}{\mathrm{d}r} + \frac{1}{r_m}(B_{13}^{kj} - B_{23}^{kj})W_j = -(\bar{I}^k r_m + \bar{I}^{kj}U_j)\omega^2 \\ &(B_{55}^{kj} - B_{13}^{jk})\frac{\mathrm{d}U_j}{\mathrm{d}r} + \frac{1}{r_m}(B_{55}^{kj} - B_{23}^{jk})U_j + D_{55}^{kj}\frac{\mathrm{d}^2W_j}{\mathrm{d}r^2} + \frac{1}{r_m}D_{55}^{kj}\frac{\mathrm{d}W_j}{\mathrm{d}r} - A_{33}^{kj}W_j = 0 \end{aligned} \tag{19}$$

It is seen that the variable r in the coefficients of Eqs. (18) is replaced by the mean radius of mth ring (r_m). Hence, in each numerical ring we have a system of two coupled second-order ordinary differential equations with constant coefficients.

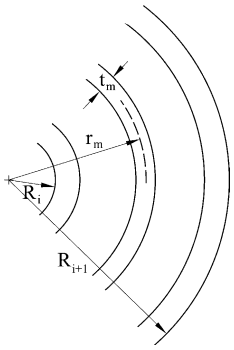

Fig. 2. Numerical rings in the ith physical ring.

The numerical results indicate, however, that there exist repeated zero roots (or eigenvalues) in the characteristic equation of the set of equations in (19). In order to enhance the solution scheme of these equations, some small artificial terms will be added to these equations so that the characteristic roots become all distinct (see Tahani and Nosier, 2004). Therefore, Eqs. (19) for the mth numerical ring are rewritten as follows:

$$\begin{aligned} &D_{11}^{kj}\frac{\mathrm{d}^2U_j}{\mathrm{d}r^2}+\frac{1}{r_m}D_{11}^{kj}\frac{\mathrm{d}U_j}{\mathrm{d}r}-\left(\frac{1}{r_m^2}D_{22}^{kj}+A_{55}^{kj}\right)U_j+(B_{13}^{kj}-B_{55}^{jk})\frac{\mathrm{d}W_j}{\mathrm{d}r}+\frac{1}{r_m}(B_{13}^{kj}-B_{23}^{kj})W_j \\ &\quad=-(\bar{I}^k r_m+\bar{I}^{kj}U_j)\omega^2+\alpha^{kj}U_j \\ &(B_{55}^{kj}-B_{13}^{jk})\frac{\mathrm{d}U_j}{\mathrm{d}r}+\frac{1}{r_m}(B_{55}^{kj}-B_{23}^{jk})U_j+D_{55}^{kj}\frac{\mathrm{d}^2W_j}{\mathrm{d}r^2}+\frac{1}{r_m}D_{55}^{kj}\frac{\mathrm{d}W_j}{\mathrm{d}r}-A_{33}^{kj}W_j=\alpha^{kj}W_j \end{aligned} \tag{20}$$

where, here, for convenience α^{kj} is assumed to have the following form:

$$\alpha^{kj}=\alpha\int_{-h/2}^{h/2}\Phi_k\Phi_j\,\mathrm{d}z \tag{21}$$

with α being a prescribed number such that α^{kj}'s in Eq. (21) are relatively small compared to the numerical values of stiffnesses A_{pq}^{kj} ($pq=33, 55$) and $D_{22}^{kj}/R_{\mathrm{O}}^2$. It should be mentioned here that α^{kj} is chosen to have a form similar to the mass terms I^{kj} appearing in the equations of motion of laminated plate within Reddy's LWT, with the density function ρ appearing in I^{kj} being replaced here by the small parameter α (see Nosier et al., 1993). This way the solution of the equations in (20) will extremely be insensitive to the small number chosen for the parameter α. Next, in order to solve Eqs. (20), for convenience the following state space variables are introduced:

$$\begin{aligned} &\{Z_1(r)\}^{(m)}=\{U(r)\}^{(m)},\quad \{Z_2(r)\}^{(m)}=\left\{\frac{\mathrm{d}U}{\mathrm{d}r}\right\}^{(m)}=\left\{\frac{\mathrm{d}Z_1}{\mathrm{d}r}\right\}^{(m)} \\ &\{Z_3(r)\}^{(m)}=\{W(r)\}^{(m)},\quad \{Z_4(r)\}^{(m)}=\left\{\frac{\mathrm{d}W}{\mathrm{d}r}\right\}^{(m)}=\left\{\frac{\mathrm{d}Z_3}{\mathrm{d}r}\right\}^{(m)} \end{aligned} \tag{22}$$

where, for example,

$$\{Z_1\}^{T(m)}=[U_1,U_2,\ldots,U_{N+1}]^{(m)} \tag{23}$$

with $\{Z_2\}^{(m)}$ through $\{Z_4\}^{(m)}$ being defined similarly as in (23). Substitution of Eqs. (22) into Eqs. (20) results in a system of $4(N+1)$ coupled first-order ordinary differential equations which may be presented as

$$\left\{\frac{\mathrm{d}Z}{\mathrm{d}r}\right\}^{(m)} = [A]^{(m)}\{Z\}^{(m)} + \{F\}^{(m)} \tag{24}$$

where

$$\{Z\}^{T(m)} = [\{Z_1\}^{T(m)}, \{Z_2\}^{T(m)}, \{Z_3\}^{T(m)}, \{Z_4\}^{T(m)}] \tag{25}$$

In Eq. (24) the coefficient matrix $[A]^{(m)}$ and vector $\{F\}^{(m)}$ are given in Appendix A. The general solutions of Eq. (24) are given by

$$\{Z\}^{(m)} = [\mathbf{U}]^{(m)}[Q(r)]^{(m)}\{K\}^{(m)} - ([A]^{-1})^{(m)}\{F\}^{(m)} \tag{26}$$

where

$$[Q(r)]^{(m)} = \mathrm{diag}(e^{\lambda_1 r}, e^{\lambda_2 r}, \ldots, e^{\lambda_{4(N+1)} r})^{(m)} \tag{27}$$

with $\{K\}^{(m)}$ being $4(N+1)$ arbitrary unknown constants. In Eqs. (26) and (27) $[\mathbf{U}]^{(m)}$ and λ_k ($k = 1, 2, \ldots, 4(N+1)$) are, respectively, the matrix of eigenvectors and eigenvalues of the coefficient matrix $[A]^{(m)}$ which, in general, must be regarded to have complex values.

Next, it is assumed that the complete disk, composed of several nested physical rings, is divided into $\bar{m}$ numerical rings. For each of them, there exists a boundary-value problem as in Eqs. (20) with the solution in Eq. (24). Therefore, there are $4\bar{m}(N+1)$ unknown constants of integrations. In order to determine these constants, the following continuity and equilibrium conditions at the interfaces of physical or numerical rings must be satisfied:

The displacement continuity conditions:

$$U_k\big|_{r=r_m+\frac{t_m}{2}} = U_k\big|_{r=r_{m+1}-\frac{t_{m+1}}{2}}, \quad W_k\big|_{r=r_m+\frac{t_m}{2}} = W_k\big|_{r=r_{m+1}-\frac{t_{m+1}}{2}} \tag{28a}$$

The stress equilibrium conditions:

$$M_r^k\big|_{r=r_m+\frac{t_m}{2}} = M_r^k\big|_{r=r_{m+1}-\frac{t_{m+1}}{2}}, \quad R_r^k\big|_{r=r_m+\frac{t_m}{2}} = R_r^k\big|_{r=r_{m+1}-\frac{t_{m+1}}{2}} \tag{28b}$$

where t_m is defined in Fig. 2. Using the definitions of stress resultants in (16), the continuity and equilibrium conditions in Eqs. (28a) and (28b) are readily presented as

$$[B]^{(m)}\{Z\}^{(m)}\Big|_{r=r_m+\frac{t_m}{2}} = [B]^{(m+1)}\{Z\}^{(m+1)}\Big|_{r=r_{m+1}-\frac{t_{m+1}}{2}} \tag{29}$$

where $[B]^{(m)}$ is given in Appendix A and $[B]^{(m+1)}$ is defined similarly.

In order to satisfy the conditions in (29), it is appropriate to use the transfer matrix method to save some computational time. Thus, we substitute Eq. (26) into Eq. (29) to obtain

$$[C]^{(m)}\{K\}^{(m)} = [C]^{(m+1)}\{K\}^{(m+1)} + \{D\}^{(m)} - \{D\}^{(m+1)} \tag{30}$$

In Eq. (30) the coefficient matrices $[C]^{(m)}$ and $[C]^{(m+1)}$ and vectors $\{D\}^{(m)}$ and $\{D\}^{(m+1)}$ are presented in Appendix A. Eq. (30) may be rewritten as

$$\{K\}^{(m)} = [S]^{(m)}\{K\}^{(m+1)} + \{T\}^{(m)} \tag{31}$$

where

$$\begin{aligned} [S]^{(m)} &= ([C]^{-1})^{(m)}[C]^{(m+1)} \\ \{T\}^{(m)} &= ([C]^{-1})^{(m)}(\{D\}^{(m)} - \{D\}^{(m+1)}) \end{aligned} \tag{32}$$

Eq. (31) may be written for each numerical ring ($m = 1, 2, \ldots, \bar{m}$) as follows:

$$\begin{aligned}
\{K\}^{(1)} &= [S]^{(1)}\{K\}^{(2)} + \{T\}^{(1)} \\
\{K\}^{(2)} &= [S]^{(2)}\{K\}^{(3)} + \{T\}^{(2)} \\
&\vdots \\
\{K\}^{(\bar{m}-1)} &= [S]^{(\bar{m}-1)}\{K\}^{(\bar{m})} + \{T\}^{(\bar{m}-1)}
\end{aligned} \tag{33}$$

Hence, by the process of elimination, we can express $\{K\}^{(1)}$ in terms of $\{K\}^{(\bar{m})}$ as

$$\{K\}^{(1)} = [S]\{K\}^{\bar{m}} + \{T\} \tag{34}$$

where the transfer matrix $[S]$ and vector $\{T\}$ are given in Appendix A.

In addition to the continuity and equilibrium conditions at the interfaces of adjacent physical and numerical rings, the boundary conditions at $r = R_I$ and $r = R_O$ must be satisfied. The clamped and free boundary conditions are defined as follows:

The clamped conditions:

$$U_k = W_k = 0 \tag{35a}$$

The traction free conditions:

$$M_r^k = R_r^k = 0 \tag{35b}$$

The boundary conditions in Eqs. (35a) and (35b), for example, in a CF (clamped at $r = R_I$ and free at $r = R_O$) disk, using Eq. (26) may readily be presented as

$$[BC]^{(1)}[\mathbf{U}]^{(1)}[Q(R_I)]^{(1)}\{K\}^{(1)} = [BC]^{(1)}([A]^{-1})^{(1)}\{F\}^{(1)} \tag{36a}$$

$$[BC]^{(\bar{m})}[\mathbf{U}]^{(\bar{m})}[Q(R_O)]^{(\bar{m})}\{K\}^{(\bar{m})} = [BC]^{(\bar{m})}([A]^{-1})^{(\bar{m})}\{F\}^{(\bar{m})} \tag{36b}$$

In Eqs. (36a) and (36b) the coefficient matrices $[BC]^{(1)}$ and $[BC]^{(\bar{m})}$ are presented in Appendix A. Next, substitution of Eq. (34) into (36a) results in

$$[BC]^{(1)}[\mathbf{U}]^{(1)}[Q(R_I)]^{(1)}[S]\{K\}^{(\bar{m})} = [BC]^{(1)}([A]^{-1})^{(1)}\{F\}^{(1)} - [BC]^{(1)}[\mathbf{U}]^{(1)}[Q(R_I)]^{(1)}\{T\} \tag{37}$$

The constants of integration $\{K\}^{(\bar{m})}$ are determined from Eqs. (36b) and (37). The other constants of integration $\{K\}^{(1)}$, $\{K\}^{(2)}, \ldots,$ $\{K\}^{(\bar{m}-1)}$ are then determined by using Eq. (31).

4. Numerical results and discussions

In what follows two numerical examples are considered. It is assumed that the hybrid rotating annular disk is constructed of a Kevlar/epoxy ring shrink-fitted over an S-2 glass/epoxy ring and that both rings are circumferentially wound. The inner and outer radii of the disks are $R_I = 5$ h and $R_O = 10$ h, respectively, with $h = 0.01$ m and it is assumed that the disks rotate with a constant angular velocity $\omega = 1000$ rad/s. These small radii (relative to the disk thickness) are purposefully chosen so that the stress distributions can be shown easily without any need to zoom the plots. In this study, only the stress field resulting from centrifugal forces is calculated. Obviously, by superposition one can obtain the total stress field due to prestresses during fabrication and inertial forces. The material properties of Kevlar/epoxy in the principal material coordinate system are taken to be (Herakovich, 1998)

$$E_1 = 76.8\ \text{GPa}, \quad E_2 = E_3 = 5.5\ \text{GPa}$$
$$G_{12} = G_{13} = 2.07\ \text{GPa}, \quad G_{23} = 1.4\ \text{GPa} \tag{38}$$
$$\nu_{12} = \nu_{13} = 0.34, \quad \nu_{23} = 0.37, \quad \rho = 1380\ \text{kg/m}^3$$

Also the material properties of S-2 glass/epoxy in the principal material coordinate system are assumed to be (Herakovich, 1998):

$$E_1 = 43.5\ \text{GPa}, \quad E_2 = E_3 = 11.5\ \text{GPa},$$
$$G_{12} = G_{13} = 3.45\ \text{GPa}, \quad G_{23} = 4.12\ \text{GPa} \tag{39}$$
$$\nu_{12} = \nu_{13} = 0.27, \quad \nu_{23} = 0.4, \quad \rho = 2000\ \text{kg/m}^3$$

where the subscripts 1, 2, and 3 indicate the on-axis (i.e., principal) material coordinates.

It is noted that in the LWT each actual physical layer can be treated as if it is made of several layers. These rather imagined layers are often referred to as numerical (or mathematical) layers (see Tahani and Nosier, 2004). Clearly, as the number of numerical layers is increased, the accuracy of the results is also increased. In the present analysis, the out-of-plane stress components are determined by using Hooke's law with six numerical layers in each ring (see Tahani and Nosier, 2004) and thirty numerical rings in each physical ring. To check the correctness and accuracy of the present method, the results achieved from this theory will be compared with those obtained by utilizing the commercial finite element package of ANSYS, revision 5.4. In the latter method, the mesh is refined till no significant change in stress distributions is obtained.

The results of the present method and the finite element method are compared for two cases of rotating disks. In the first case, the disk is clamped at the inner boundary and free at the outer boundary (CF) and in the second case, the disk is free at the inner and outer boundaries (FF). Fig. 3a and b illustrate the radial displacement versus r at $z = 0$ in CF and FF rotating disks, respectively. Also the variation of the radial stress σ_r at $z = h/4$ is shown in Fig. 4. It is noted that, as it is expected, the radial stress σ_r is continuous at the interface of S-2 glass/epoxy and Kevlar/epoxy rings, but the hoop stress σ_θ at $z = h/4$ as shown in Fig. 5 is discontinuous at the interface. It can be seen from the figures that very good agreement is obtained using the mentioned method for both displacements and stresses.

The distributions of the transverse normal stress σ_z at $z = h/4$ in CF and FF disks are illustrated in Fig. 6a and b, respectively. It is seen that σ_z is nonzero and discontinuous at the interface. Finally, distributions of the transverse shear stress σ_{rz} at $z = h/4$ are displayed in Fig. 7a and b. It is seen that both σ_z and σ_{rz} have

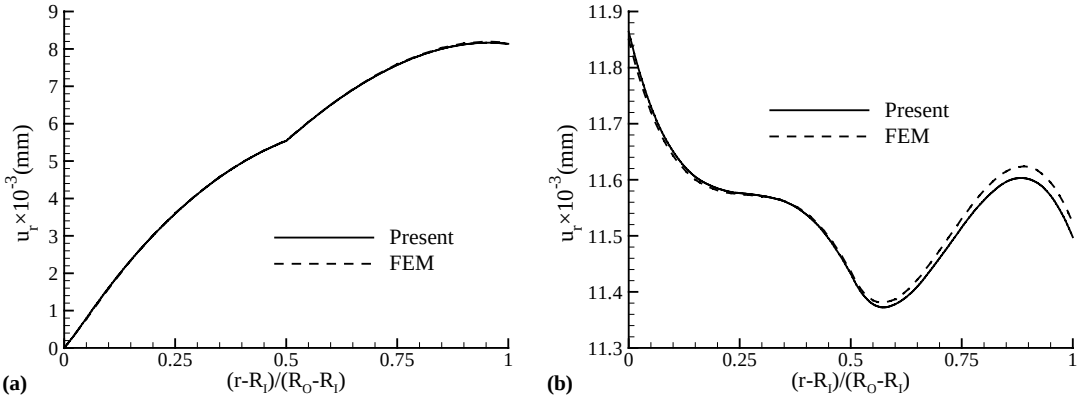

Fig. 3. Distribution of the radial displacement at $z = 0$ in (a) CF disk and (b) FF disk.

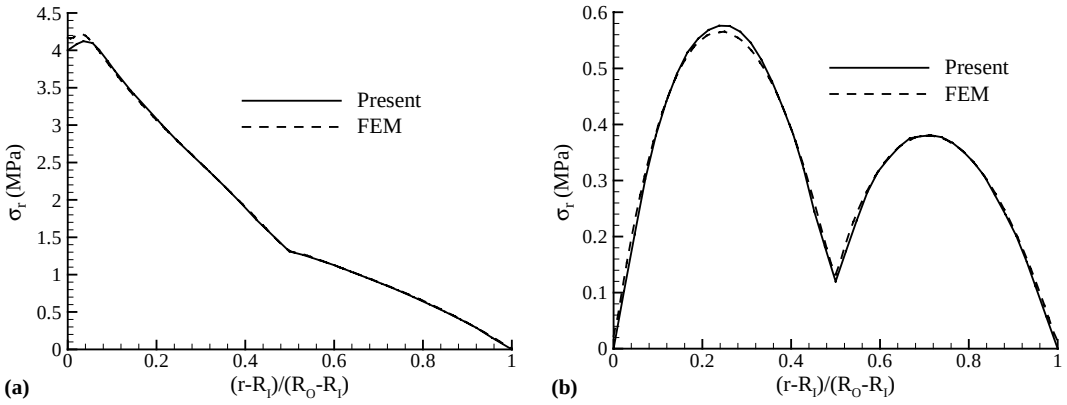

Fig. 4. Distribution of the radial stress σ_r at $z = h/4$ in (a) CF disk and (b) FF disk.

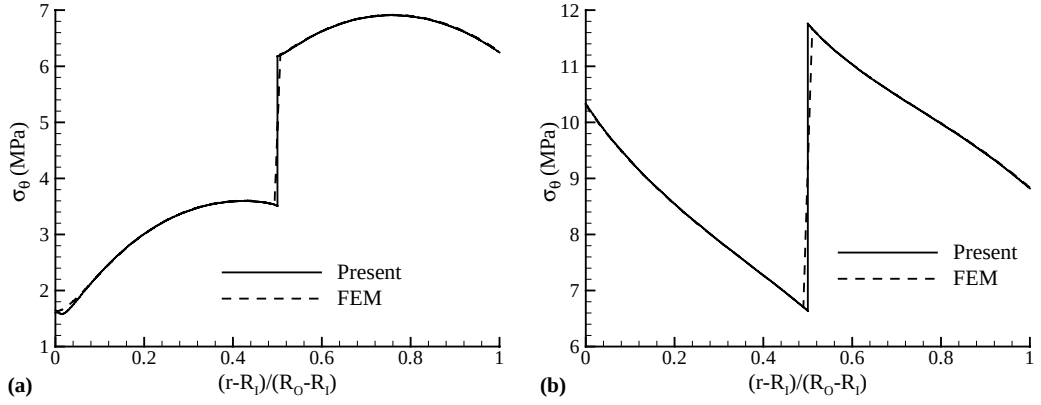

Fig. 5. Distribution of the hoop stress σ_θ at $z = h/4$ in (a) CF disk and (b) FF disk.

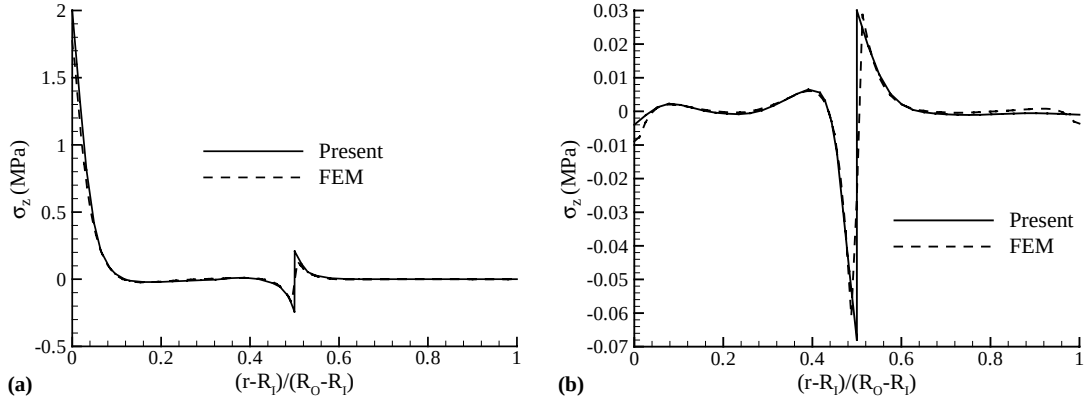

Fig. 6. Distribution of the transverse normal stress σ_z at $z = h/4$ in (a) CF disk and (b) FF disk.

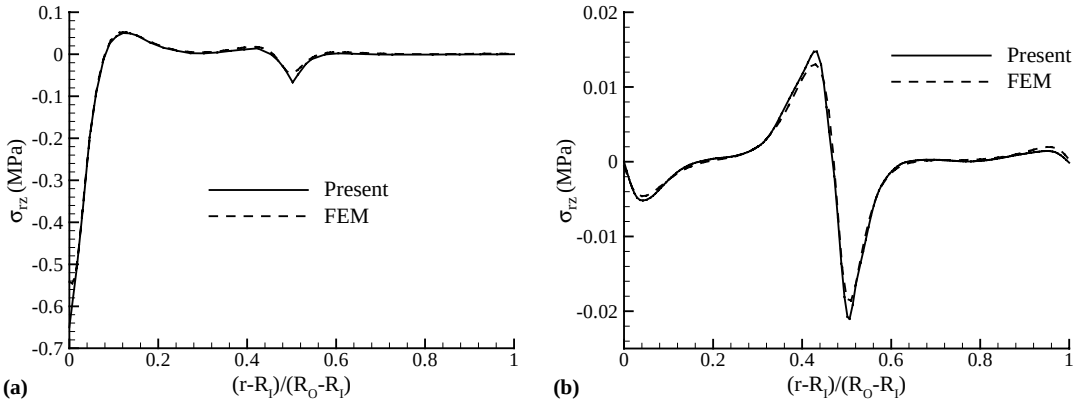

Fig. 7. Distribution of the transverse shear stress σ_{rz} at $z = h/4$ in (a) CF disk and (b) FF disk.

a large magnitude at the inner radius of the disk where there is a fixed boundary condition. Also far away from the material discontinuity in the outer ring it can be seen that the out-of-plane stresses vanish as it is expected. The current solutions are seen to closely match the finite element solutions in all regions.

5. Conclusions

Deformations and stresses in rotating annular disks composed of cylindrically orthotropic nested rings are determined by using a layerwise plate theory (LWT). It is assumed that the circular plate rotates with a constant angular velocity. Numerical results are obtained in a clamped-free and a free–free rotating disk made of two nested circumferentially wound rings. The accuracy and effectiveness of the present theory in describing the localized three-dimensional effects are demonstrated by comparing the results of the LWT with those obtained by a finite element method. The results indicate that the stress field is three-dimensional in regions close to the sudden transition of material properties and must be considered in design of such structures with this kind of discontinuity. The method could serves as a useful tool in the analysis of a material discontinuity in an initial design situation.

Appendix A

The coefficient matrix $[A]^{(m)}$ and vector $\{F\}^{(m)}$ appearing in Eq. (24) are defined as

$$[A]^{(m)} = \begin{bmatrix} [0] & [I] & [0] & [0] \\ [a_1] & [a_2] & [a_3] & [a_4] \\ [0] & [0] & [0] & [I] \\ [b_1] & [b_2] & [b_3] & [b_4] \end{bmatrix}, \quad \{F\}^{(m)} = \begin{Bmatrix} \{0\} \\ \{a_5\} \\ \{0\} \\ \{0\} \end{Bmatrix}$$

where $[0]$ and $[I]$ are $(N+1)\times(N+1)$ square zero and identity matrices, respectively, and $\{0\}$ is a zero vector with $N+1$ rows. The remaining matrices in the above equations are as follows:

$$[a_1] = [D_{11}]^{-1}\left(\frac{1}{r_m^2}[D_{22}] + [A_{55}] - [\overline{I}]\omega^2 + [\alpha]\right)$$

$$[a_2] = -\frac{1}{r_m}[I]$$

$$[a_3] = \frac{1}{r_m}[D_{11}]^{-1}([B_{23}] - [B_{13}])$$

$$[a_4] = [D_{11}]^{-1}([B_{55}]^{\mathrm{T}} - [B_{13}])$$

$$\{a_5\} = -[D_{11}]^{-1}\{\bar{I}\}r_m\omega^2$$

$$[b_1] = \frac{1}{r_m}[D_{55}]^{-1}([B_{23}]^{\mathrm{T}} - [B_{55}])$$

$$[b_2] = [D_{55}]^{-1}([B_{13}]^{\mathrm{T}} - [B_{55}])$$

$$[b_3] = [D_{55}]^{-1}([A_{33}] + [\alpha])$$

$$[b_4] = -\frac{1}{r_m}[I]$$

where $[\bar{I}]$ and $\{\bar{I}\}$ are the matrix and vector of mass terms defined in Eq. (12). Also, the coefficient matrix $[B]^{(m)}$ appearing in Eq. (29) is defined as

$$[B]^{(m)} = \begin{bmatrix} [I] & [0] & [0] & [0] \\ [0] & [0] & [I] & [0] \\ \frac{1}{r_m + \frac{t_m}{2}}[D_{12}] & [D_{11}] & [B_{13}] & [0] \\ [B_{55}] & [0] & [0] & [D_{55}] \end{bmatrix}$$

The coefficient matrices in Eq. (30) are defined as follows:

$$[C]^{(m)} = [B]^{(m)}[\mathbf{U}]^{(m)}\left[Q\left(r_m + \frac{t_m}{2}\right)\right]^{(m)}$$

$$[C]^{(m+1)} = [B]^{(m+1)}[\mathbf{U}]^{(m+1)}\left[Q\left(r_{m+1} - \frac{t_{m+1}}{2}\right)\right]^{(m+1)}$$

$$\{D\}^{(m)} = [B]^{(m)}([A]^{-1})^{(m)}\{F\}^{(m)}$$

$$\{D\}^{(m+1)} = [B]^{(m+1)}([A]^{-1})^{(m+1)}\{F\}^{(m+1)}$$

The coefficient matrices in Eq. (31) are given by

$$[S] = [S]^{(1)}[S]^{(2)}\cdots[S]^{(\bar{m}-1)}$$
$$\{T\} = \{T\}^{(1)} + [S]^{(1)}\{T\}^{(2)} + \cdots + [S]^{(1)}[S]^{(2)}\cdots[S]^{(\bar{m}-2)}\{T_m\}^{(\bar{m}-1)}$$

The coefficient matrices appearing in Eqs. (36a) and (36b) are defined as

$$[BC]^{(1)} = \begin{bmatrix} [I] & [0] & [0] & [0] \\ [0] & [0] & [I] & [0] \end{bmatrix}$$

$$[BC]^{(\bar{m})} = \begin{bmatrix} \frac{1}{R_O}[D_{12}] & [D_{11}] & [B_{13}] & [0] \\ [B_{55}] & [0] & [0] & [D_{55}] \end{bmatrix}$$

References

Arnold, S.M., Saleeb, A.F., Al-Zoubi, N.R., 2002. Deformation and life analysis of composite flywheel disk systems. Composites Part B: Engineering 33, 433–459.

Bert, C.W., 1975. Centrifugal stresses in arbitrarily laminated, rectangular-anisotropic circular discs. Journal of Strain Analysis 10 (2), 84–92.

Christensen, R.M., Wu, E.M., 1977. Optimal design of anisotropic (fiber-reinforced) flywheels. Journal of Composite Materials 11, 395–404.

Durodola, J.F., Attia, O., 2000. Deformation and stresses in functionally graded rotating disks. Composite Science and Engineering 60, 987–995.

Foral, R.F., Newhouse, N.L., 1980. On the performance of hoop wound composite flywheel rotors. In: Flywheel Technology Symposium, Scottsdale, AZ.

Fung, Y.C., 1965. Foundations of Solid Mechanics, first ed. Prentice-Hall, Englewood Cliffs, NJ.

Genta, G., Gola, M., 1981. The stress distribution in orthotropic rotating disks. Journal of Applied Mechanics 48, 559–562.

Gurushankar, G.V., 1975. Thermal stresses in a rotating nonhomogeneous, anisotropic disk of varying thickness and density. Journal of Strain Analysis 10, 137–142.

Herakovich, C.T., 1998. Mechanics of fibrous composites. Wiley, New York.

Jain, R., Ramachandra, K., Simha, K.R.Y., 2000. Singularity in rotating orthotropic discs and shells. International Journal of Solids and Structures 37, 2035–2058.

Lekhnitskii, S.G., 1981. Theory of elasticity of an anisotropic body. Mir Publishers.

Nosier, A., Kapania, R.K., Reddy, J.N., 1993. Free vibration analysis of laminated plates using a layerwise theory. AIAA Journal 31 (12), 2335–2346.

Reddy, T.Y., Srinath, H., 1974. Elastic stresses in a rotating anisotropic annular disk of variable thickness and variable density. International Journal of Solids and Structures 16, 85–89.

Tahani, M., Nosier, A., 2004. Accurate determination of interlaminar stresses in general cross-ply laminates. Mechanics of Advanced Materials and Structures 11 (1), 67–92.

Timoshenko, S.P., Goodier, J.N., 1970. Theory of Elasticity, third ed. McGraw-Hill.

Tutuncu, N., 1995. Effect of anisotropy on stresses in rotating discs. International Journal of Mechanical Sciences 37 (8), 873–881.

Tutuncu, N., 1998. Interlaminar thermal stresses in polar-anisotropic circular plates. Journal of Reinforced Plastics and Composites 17 (11), 1024–1035.